

PDF hosted at the Radboud Repository of the Radboud University Nijmegen

The following full text is a publisher's version.

For additional information about this publication click this link.

<http://hdl.handle.net/2066/29890>

Please be advised that this information was generated on 2019-04-25 and may be subject to change.

Enhanced passive Ca^{2+} reabsorption and reduced Mg^{2+} channel abundance explains thiazide-induced hypocalciuria and hypomagnesemia

Tom Nijenhuis,¹ Volker Vallon,² Annemiete W.C.M. van der Kemp,¹ Johannes Loffing,³ Joost G.J. Hoenderop,¹ and René J.M. Bindels¹

¹Department of Physiology, Nijmegen Centre for Molecular Life Sciences, Radboud University Nijmegen Medical Centre, Nijmegen, The Netherlands.

²Departments of Medicine and Pharmacology, University of California and Veterans Affairs Medical Center, San Diego, California, USA.

³Department of Medicine, Unit of Anatomy, University of Fribourg, Fribourg, Switzerland.

Thiazide diuretics enhance renal Na^+ excretion by blocking the $\text{Na}^+\text{-Cl}^-$ cotransporter (NCC), and mutations in NCC result in Gitelman syndrome. The mechanisms underlying the accompanying hypocalciuria and hypomagnesemia remain debated. Here, we show that enhanced passive Ca^{2+} transport in the proximal tubule rather than active Ca^{2+} transport in distal convoluted tubule explains thiazide-induced hypocalciuria. First, micropuncture experiments in mice demonstrated increased reabsorption of Na^+ and Ca^{2+} in the proximal tubule during chronic hydrochlorothiazide (HCTZ) treatment, whereas Ca^{2+} reabsorption in distal convoluted tubule appeared unaffected. Second, HCTZ administration still induced hypocalciuria in transient receptor potential channel subfamily V, member 5–knockout (Trpv5–knockout) mice, in which active distal Ca^{2+} reabsorption is abolished due to inactivation of the epithelial Ca^{2+} channel Trpv5. Third, HCTZ upregulated the Na^+/H^+ exchanger, responsible for the majority of Na^+ and, consequently, Ca^{2+} reabsorption in the proximal tubule, while the expression of proteins involved in active Ca^{2+} transport was unaltered. Fourth, experiments addressing the time-dependent effect of a single dose of HCTZ showed that the development of hypocalciuria parallels a compensatory increase in Na^+ reabsorption secondary to an initial natriuresis. Hypomagnesemia developed during chronic HCTZ administration and in NCC–knockout mice, an animal model of Gitelman syndrome, accompanied by downregulation of the epithelial Mg^{2+} channel transient receptor potential channel subfamily M, member 6 (Trpm6). Thus, Trpm6 downregulation may represent a general mechanism involved in the pathogenesis of hypomagnesemia accompanying NCC inhibition or inactivation.

Introduction

Thiazide diuretics are among the most commonly prescribed drugs, particularly in the treatment of arterial hypertension. These diuretics enhance renal Na^+ excretion through inhibition of the $\text{Na}^+\text{-Cl}^-$ cotransporter (NCC) present in the apical membrane of distal convoluted tubule (DCT) cells (1). In addition, these drugs are known to affect the Ca^{2+} and Mg^{2+} balance, inducing hypocalciuria and hypomagnesemia, respectively (2–7). Consequently, thiazides are frequently used in the treatment of idiopathic hypercalciuria and nephrolithiasis, disorders with a high incidence and socioeconomic burden in Western society (8–10). Furthermore, mutations in the gene encoding NCC have been shown to cause Gitelman syndrome, a recessive disorder with a phenotype that resembles the effects of chronic thiazide administration characterized by hypocalciuria, renal Mg^{2+} wasting, and hypomagnese-

mia (4, 6, 11, 12). Intriguingly, the molecular mechanisms responsible for the hypocalciuria and hypomagnesemia during thiazide administration and Gitelman syndrome remain elusive.

Two hypotheses prevail with respect to the Ca^{2+} -sparing effect of thiazides (2, 4, 5, 13). First, renal salt and water loss due to thiazide treatment result in contraction of the extracellular volume (ECV), which triggers a compensatory increase in proximal Na^+ reabsorption. This would in turn enhance the electrochemical gradient, driving passive Ca^{2+} transport in the proximal tubule (1, 14). According to this line of reasoning, thiazide-induced hypocalciuria results from enhancement of passive paracellular Ca^{2+} reabsorption secondary to ECV contraction (2, 4, 7, 15). Second, microperfusion experiments suggested that acute administration of thiazides in the tubular lumen stimulates Ca^{2+} reabsorption in the distal convoluted tubule accessible to micropuncture (3). These accessible segments primarily consist of distal aspects of NCC-expressing DCT (DCT2) as well as low- or non-NCC-expressing connecting tubule (CNT). Subsequently, several molecular mechanisms were postulated to explain this latter stimulatory effect (2, 4, 5, 16). These include hyperpolarization of the luminal plasma membrane and/or enhanced basolateral $\text{Na}^+/\text{Ca}^{2+}$ exchange due to a decreased intracellular Na^+ concentration, both of which may increase apical Ca^{2+} entry through the epithelial Ca^{2+} channel transient receptor potential channel subfamily V, member 5 (Trpv5),

Nonstandard abbreviations used: C_{Cr} , creatinine clearance; C_{Li} , lithium clearance; CNT, connecting tubule; DCT, distal convoluted tubule; ECV, extracellular volume; HCTZ, hydrochlorothiazide; NCC, $\text{Na}^+\text{-Cl}^-$ cotransporter; NCX1 , $\text{Na}^+/\text{Ca}^{2+}$ exchanger 1; NHE3 , Na^+/H^+ exchanger 3; NKCC2 , $\text{Na}^+\text{-K}^+\text{-2Cl}^-$ cotransporter 2; TAL, thick ascending limb of Henle; Trpm6, transient receptor potential channel subfamily M, member 6; Trpv5, transient receptor potential channel subfamily V, member 5.

Conflict of interest: The authors have declared that no conflict of interest exists.

Citation for this article: *J. Clin. Invest.* 115:1651–1658 (2005). doi:10.1172/JCI24134.



Table 1

Urine analysis of vehicle and HCTZ-treated *Trpv5^{+/+}* and *Trpv5^{-/-}* mice

	<i>Trpv5^{+/+}</i>		<i>Trpv5^{-/-}</i>	
	Controls	HCTZ	Controls	HCTZ
Urine volume (ml/24 h)	5.2 ± 0.9	6.9 ± 1.4 ^A	13.0 ± 1.7	10.8 ± 0.2
Ca ²⁺ excretion (μmol/24 h)	41 ± 2	34 ± 2 ^A	273 ± 10	169 ± 13 ^B
Ca ²⁺ /creatinine	0.29 ± 0.02	0.15 ± 0.02 ^A	1.96 ± 0.06	1.17 ± 0.14 ^B
Mg ²⁺ excretion (μmol/24 h)	26 ± 14	85 ± 9 ^A	nd	nd
Mg ²⁺ /creatinine	0.2 ± 0.1	0.6 ± 0.1 ^A	nd	nd
Na ⁺ excretion (μmol/24 h)	751 ± 67	757 ± 50	780 ± 25	777 ± 11
Urinary pH	7.1 ± 0.1	6.8 ± 0.2	6.0 ± 0.1	6.9 ± 0.1 ^B
C _{Cr} (ml/min)	0.24 ± 0.04	0.24 ± 0.01	0.27 ± 0.01	0.26 ± 0.03
C _{Li} (μl/min)	13.5 ± 0.6	9.8 ± 0.2 ^A	13.9 ± 0.7	10.1 ± 0.5 ^A

Controls, animals receiving vehicle only; HCTZ, animals receiving 25 mg/kg/d HCTZ; nd, not determined. Data are presented as mean ± SEM. ^A*P* < 0.05 versus vehicle-treated *Trpv5^{+/+}*; ^B*P* < 0.05 versus vehicle-treated *Trpv5^{-/-}*.

the expression of which is restricted to DCT2 and the CNT (15–19). Similar mechanisms were proposed to explain the hypocalciuria in Gitelman syndrome (4, 5).

Hypomagnesemia has been suggested to result from K⁺ deficiency, increased passive Mg²⁺ secretion, or decreased active Mg²⁺ transport in the DCT (5, 6, 20). However, experimental evidence for either hypothesis is lacking. Studies have been seriously hampered by the fact that the exact mechanism responsible for active Mg²⁺ reabsorption has not been identified. Transient receptor potential channel subfamily M, member 6 (Trpm6) was recently identified as a Mg²⁺-permeable channel predominantly expressed along the apical membrane of the DCT (21–23). Mutations in Trpm6 were shown to cause autosomal recessive hypomagnesemia, characterized by inappropriately high fractional Mg²⁺ excretion rates and disturbed intestinal Mg²⁺ absorption (21, 22). This clearly suggested that Trpm6 constitutes the apical entry step in active Mg²⁺ (re)absorption and provides an important new tool for studying this process on a molecular level.

Recently, transgenic mouse models were developed that might offer new insights into the pathogenesis of hypocalciuria and hypomagnesemia during thiazide treatment and in Gitelman syndrome. We generated *Trpv5*-knockout (*Trpv5^{-/-}*) mice by ablation of the *Trpv5* gene (24). These mice showed robust renal Ca²⁺ wasting, and micropuncture experiments illustrated that active Ca²⁺ reabsorption in distal convoluted is effectively abolished. Thus, *Trpv5^{-/-}* mice constitute a unique mouse model that can be used to unravel the relative contribution of passive and active Ca²⁺ reabsorption in thiazide-induced hypocalciuria. Furthermore, Schultheis et al. generated *NCC*-knockout (*NCC^{-/-}*) mice exhibiting both hypocalciuria and hypomagnesemia, which represent a valuable animal model that mimics Gitelman syndrome (25).

The aim of the present study was to elucidate the molecular mechanisms responsible for hypocalciuria and hypomagnesemia accompanying *NCC* inactivation. The effect of chronic hydrochlorothiazide (HCTZ) treatment and the time-dependent effect of a single dose of HCTZ on urinary Ca²⁺ and Mg²⁺ excretion was evaluated in wild-type and *Trpv5^{-/-}* mice. Tubular Na⁺ and Ca²⁺ handling was assessed by in vivo free-flow micropuncture experiments in control and HCTZ-treated wild-type

mice. In addition, an extensive evaluation of the renal expression level of Na⁺, Ca²⁺, and Mg²⁺ transport proteins was performed in vehicle and HCTZ-treated wild-type and *Trpv5^{-/-}* mice. Moreover, the renal expression of the epithelial Mg²⁺ channel Trpm6 was assessed in *NCC^{-/-}* mice.

Results

Metabolic studies in HCTZ-treated Trpv5^{+/+} and Trpv5^{-/-} mice. The metabolic data obtained during chronic administration of HCTZ (25 mg/kg/d during 6 days) in *Trpv5^{+/+}* and *Trpv5^{-/-}* mice are shown in Tables 1 and 2. Genetic ablation of *Trpv5* in mice resulted in a calciuria that was about 6-fold higher than that in *Trpv5^{+/+}* mice (Table 1) (24). Importantly, HCTZ treatment significantly decreased urinary Ca²⁺ excretion in *Trpv5^{+/+}* as well as *Trpv5^{-/-}* mice. Serum Ca²⁺ levels were not affected by HCTZ in *Trpv5^{+/+}* mice but significantly increased in *Trpv5^{-/-}*

mice. In addition, HCTZ treatment significantly enhanced urinary Mg²⁺ excretion in *Trpv5^{+/+}* mice. Serum Mg²⁺ levels were significantly reduced in HCTZ-treated wild-type mice. Urine volume was increased by HCTZ treatment in the *Trpv5^{+/+}* mice, whereas diuresis in HCTZ-treated *Trpv5^{-/-}* mice did not differ from that in non-treated controls. Furthermore, overall Na⁺ excretion was unaltered by chronic HCTZ treatment in wild-type as well as *Trpv5^{-/-}* mice, and GFR was not affected, as shown by the creatinine clearance (C_{Cr}). HCTZ treatment significantly decreased endogenous lithium clearance (C_{Li}), an inverse measure of proximal tubular Na⁺ reabsorption and, thereby, passive paracellular Ca²⁺ transport in the proximal tubule. Urinary pH was not affected by HCTZ treatment in wild-type mice, whereas HCTZ neutralized the acidic urinary pH in *Trpv5^{-/-}* mice. HCTZ significantly increased hematocrit in *Trpv5^{+/+}* and *Trpv5^{-/-}* mice, and body weight was reduced compared with their respective controls (Table 2). Serum Na⁺, K⁺, and creatinine levels were not influenced by HCTZ treatment.

Renal mRNA and protein expression of Ca²⁺, Mg²⁺, and Na⁺ transporters. Ca²⁺, Mg²⁺, and Na⁺ transport protein mRNA expression levels were determined by real-time quantitative PCR analysis, and protein abundance was determined by immunohistochemistry (Figures 1 and 2). HCTZ did not affect the mRNA expression levels of the apically localized epithelial Ca²⁺ channel *Trpv5* in wild-type mice (Figure

Table 2

Serum analysis and body weight of vehicle and HCTZ-treated *Trpv5^{+/+}* and *Trpv5^{-/-}* mice

	<i>Trpv5^{+/+}</i>		<i>Trpv5^{-/-}</i>	
	Controls	HCTZ	Controls	HCTZ
Serum				
[Ca ²⁺] (mmol/l)	2.47 ± 0.01	2.46 ± 0.03	2.36 ± 0.02	2.44 ± 0.02 ^B
[Mg ²⁺] (mmol/l)	0.86 ± 0.01	0.80 ± 0.01 ^A	nd	nd
[Na ⁺] (mmol/l)	100 ± 4	104 ± 3	100 ± 1	103 ± 3
[K ⁺] (mmol/l)	5.2 ± 0.2	5.3 ± 0.1	5.1 ± 0.1	5.1 ± 0.1
[Creatinine] (μmol/l)	34 ± 1	36 ± 1	37 ± 1	35 ± 1
Hematocrit (%)	52 ± 1	57 ± 1 ^A	52 ± 1	55 ± 1 ^B
Weight loss (mg)	1.0 ± 0.1	1.5 ± 0.1 ^A	0.2 ± 0.1	0.7 ± 0.2 ^B

Data are presented as mean ± SEM. ^A*P* < 0.05 versus vehicle-treated *Trpv5^{+/+}*; ^B*P* < 0.05 versus vehicle-treated *Trpv5^{-/-}*.

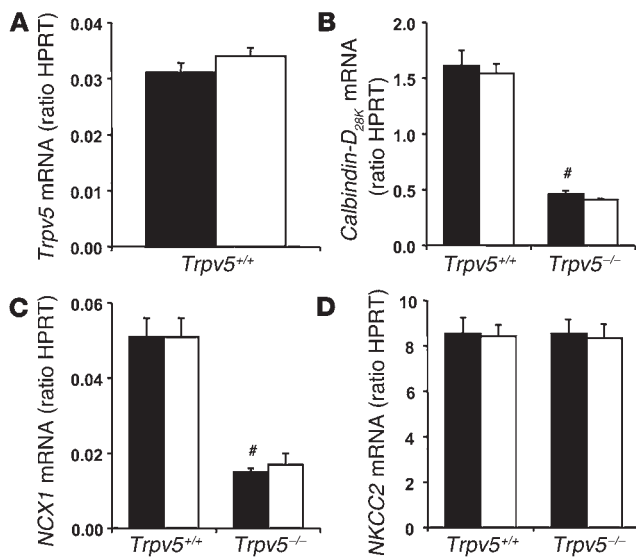


Figure 1

Effect of chronic HCTZ treatment on renal mRNA expression levels of Ca²⁺ and Na⁺ transport proteins in *Trpv5*^{+/+} and *Trpv5*^{-/-} mice. Renal mRNA expression levels of the epithelial Ca²⁺ channel *Trpv5* (A), calbindin-D_{28k} (B), NCX1 (C), and NKCC2 (D) were determined by real-time quantitative PCR analysis and are depicted as the ratio to hypoxanthine-guanine phosphoribosyl transferase (HPRT). Black bars, vehicle-treated; white bars, HCTZ-treated, 25 mg/kg/d during 6 days. *n* = 9 animals per treatment group. Data are presented as mean ± SEM. #*P* < 0.05 versus vehicle-treated *Trpv5*^{+/+}.

1A), nor did it affect *Trpv5* protein levels in the DCT and CNT (Figure 2A). Renal mRNA and protein levels of the cytosolic Ca²⁺-binding protein calbindin-D_{28k} were significantly decreased in *Trpv5*^{-/-} mice compared with their wild-type littermates (Figure 1B and Figure 2B). Likewise, mRNA expression of the basolateral Na⁺/Ca²⁺ exchanger 1 (NCX1) was reduced in these mice. However, HCTZ administration

did not significantly alter calbindin-D_{28k} and NCX1 expression in both *Trpv5*^{+/+} and *Trpv5*^{-/-} mice (Figure 1, B and C, and Figure 2B). This unaffected calbindin-D_{28k} protein expression was confirmed by semiquantitative immunoblotting (89% ± 11% and 106% ± 11% of nontreated *Trpv5*^{+/+} and *Trpv5*^{-/-} controls, respectively).

In general, passive Ca²⁺ reabsorption is driven by the electrochemical gradient generated by transcellular Na⁺ transport. Therefore, we determined Na⁺/H⁺ exchanger (NHE3) and Na⁺-K⁺-2Cl⁻ cotransporter (NKCC2) expression as indirect measures of passive paracellular Ca²⁺ transport in the proximal tubule and thick ascending limb of Henle (TAL), respectively. In accordance with the decreased C_{Li}, proximal tubular NHE3 protein expression was significantly increased in HCTZ-treated *Trpv5*^{+/+} and *Trpv5*^{-/-} mice (Figure 2D). In contrast, the level of renal NKCC2 mRNA expression, which is exclusively expressed in TAL, was not affected by HCTZ treatment (Figure 1D).

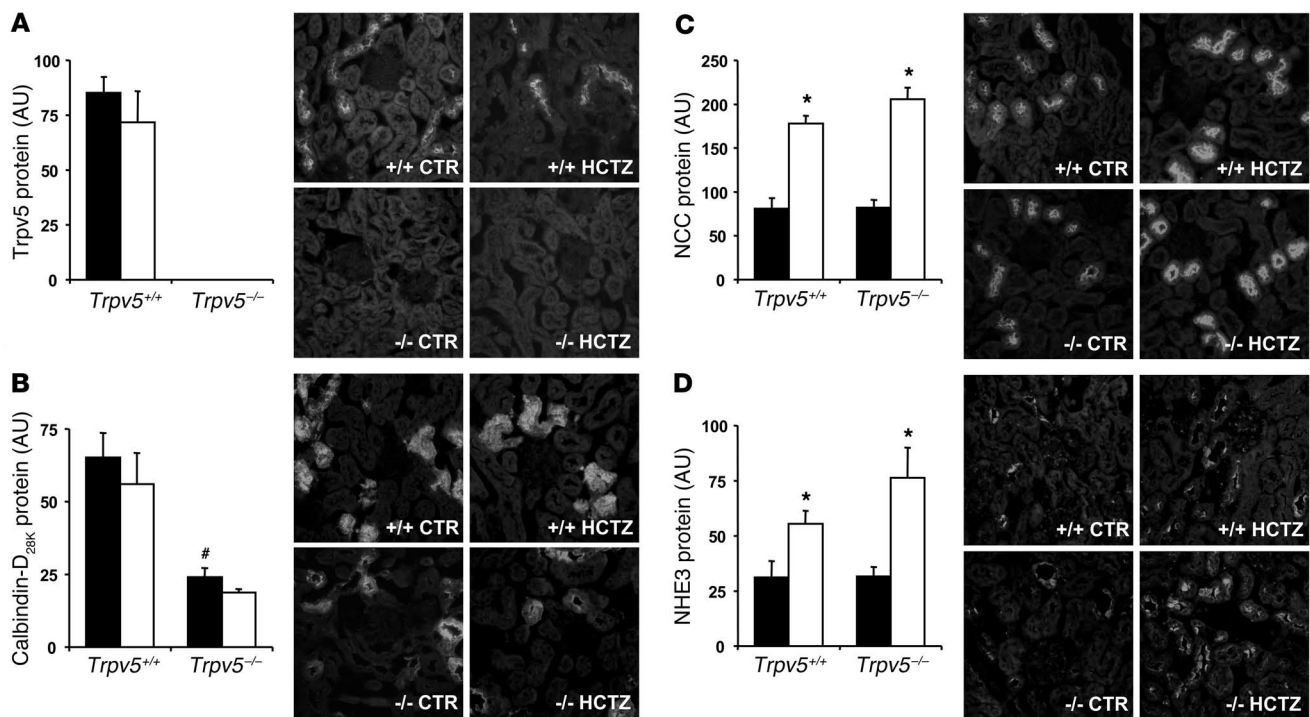


Figure 2

Effect of chronic HCTZ treatment on renal protein abundance of Ca²⁺ and Na⁺ transport proteins in *Trpv5*^{+/+} and *Trpv5*^{-/-} mice. Protein abundance was determined by computerized analysis of immunohistochemical images and is presented as integrated optical density (IOD; AU) for the epithelial Ca²⁺ channel *Trpv5* (A), calbindin-D_{28k} (B), NCC (C), and NHE3 (D). Black bars, vehicle-treated (CTR); white bars, HCTZ-treated, 25 mg/kg/d during 6 days; +/+ CTR and +/+ HCTZ, vehicle- and HCTZ-treated *Trpv5*^{+/+} mice, respectively; -/- CTR and -/- HCTZ, vehicle- and HCTZ-treated *Trpv5*^{-/-} mice, respectively. *n* = 9 animals per treatment group. Data are presented as mean ± SEM. **P* < 0.05 versus respective vehicle-treated controls; #*P* < 0.05 versus vehicle-treated *Trpv5*^{+/+}.

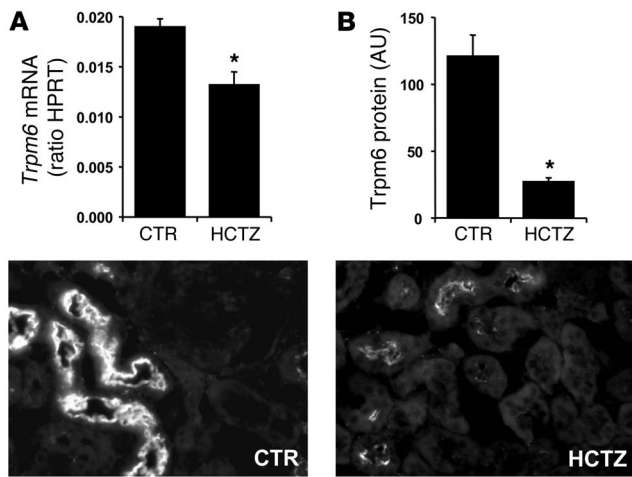


Figure 3 Effect of chronic HCTZ treatment on renal mRNA expression and protein abundance of the epithelial Mg²⁺ channel Trpm6. (A) Renal mRNA expression levels of the epithelial Mg²⁺ channel Trpm6 were determined by real-time quantitative PCR analysis and are depicted as the ratio to HPRT. (B) Trpm6 protein abundance was determined by computerized analysis of immunohistochemical images and is presented as integrated optical density (AU). HCTZ, 25 mg/kg/d HCTZ for 6 days. *n* = 9 per treatment group. Data are presented as mean ± SEM. **P* < 0.05 versus vehicle-treated controls.

Interestingly, HCTZ treatment significantly reduced mRNA expression and protein abundance of the epithelial Mg²⁺ channel Trpm6 in wild-type mice (Figure 3, A and B). To confirm the viability of the DCT and thereby the specificity of the Trpm6 downregulation, we determined NCC protein expression by immunohistochemical analysis (Figure 2C). NCC protein abundance was significantly increased in HCTZ-treated *Trpv5*^{+/+} and *Trpv5*^{-/-} mice. This was confirmed by semiquantitative immunoblotting (153% ± 20% and 143% ± 11% of nontreated *Trpv5*^{+/+} and *Trpv5*^{-/-} controls, respectively). Of note, deleterious effects or apoptotic alterations in the DCT were not detected by immunohistochemical or light microscopical analysis of HCTZ-treated mice as reported previously (7, 26).

Renal expression of the epithelial Mg²⁺ channel Trpm6 in *NCC*^{-/-} mice. Mice lacking NCC display a phenotype similar to the effects of chronic thiazide administration, including hypocalciuria and hypomagnesemia (25). Therefore, the renal expression of Trpm6 was determined in *NCC*^{+/+} and *NCC*^{-/-} mice. Renal Trpm6 mRNA expression was significantly reduced in *NCC*^{-/-} mice (Figure 4A). Furthermore, immunohistochemical analysis revealed that Trpm6 protein abundance along the apical membrane of the DCT is profoundly decreased in these mice (Figure 4B).

Time-dependent effect of a single dose of HCTZ in wild-type and *Trpv5*^{-/-} mice. To further evaluate the time-dependent effect of thiazides on Na⁺, Ca²⁺ and Mg²⁺ excretion and their interdependency, additional metabolic cage experiments were performed. Figure 5 summarizes the effect of a single dose of HCTZ on Na⁺ and Ca²⁺ excretion 6, 12, and 24 hours after administration. During the first 6 hours after HCTZ administration, Na⁺ excretion was significantly increased in *Trpv5*^{+/+} and *Trpv5*^{-/-} mice (433% ± 16% and 414% ± 17%, respectively). In contrast, the urinary excretion of Ca²⁺ was unaffected (109% ± 11% and 95% ± 3%, respectively). However, during the next

6 hours, Na⁺ excretion was significantly decreased in both HCTZ-treated *Trpv5*^{+/+} and *Trpv5*^{-/-} mice compared with their corresponding controls (54% ± 11% and 55% ± 3%, respectively). Importantly, within this latter time period a significant hypocalciuria developed in HCTZ-treated *Trpv5*^{+/+} as well as *Trpv5*^{-/-} mice (44% ± 3% and 46% ± 6%, respectively). Thus, the Ca²⁺-sparing effect resulting from a single dose of HCTZ coincides with a period of increased renal Na⁺ reabsorption. Furthermore, while absolute Ca²⁺ excretion differed between *Trpv5*^{+/+} and *Trpv5*^{-/-} mice, the overall effect of HCTZ administration was identical in *Trpv5*^{+/+} and *Trpv5*^{-/-} mice. Mg²⁺ excretion was unaffected by a single dose of HCTZ during the 24 hours after its administration (data not shown).

In vivo free-flow micropuncture studies in HCTZ-treated mice. We performed micropuncture experiments in control and HCTZ-treated (25 mg/kg/d during 6 days) wild-type mice in order to directly evaluate tubular Na⁺ and Ca²⁺ handling in response to chronic thiazide treatment. No significant differences were observed between HCTZ-treated mice and control mice with regard to mean arterial blood pressure (93 ± 4 vs. 87 ± 3 mmHg; *n* = 5–6 mice), single nephron GFR from distal (7.3 ± 0.8 vs. 6.9 ± 0.5 nl/min; *n* = 10 nephrons per group) or proximal tubular collections (6.8 ± 0.3 vs. 6.9 ± 0.3 nl/min; *n* = 17–21 nephrons per group). Similarly, the amounts of Na⁺ and Ca²⁺ filtered per nephron were not different between HCTZ-treated and control mice (1,146 ± 44 vs. 1,181 ± 50 pmol/min and 15.2 ± 0.5 vs. 15.9 ± 0.7 pmol/min, respectively). Reabsorption of Na⁺, fluid, and Ca²⁺ up to the last surface loop of the proximal tubule, however, was significantly greater in HCTZ-treated than in control mice (Figure 6A). As a consequence, the absolute delivery of Ca²⁺ to the late proximal tubule was significantly lower in HCTZ-treated mice (5.4 ± 0.4 vs. 6.9 ± 0.4 pmol/min). Absolute and fractional delivery of Ca²⁺ to the distal convolution accessible to micropuncture was likewise significantly lower in HCTZ-treated versus control mice (0.21 ± 0.03 vs. 0.71 ± 0.18 pmol/min and

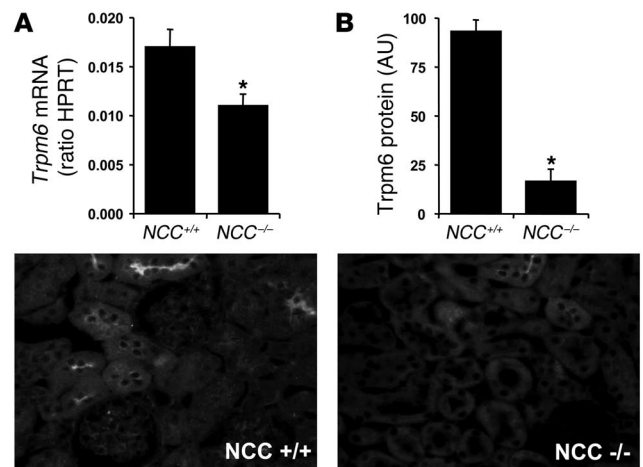


Figure 4 Renal mRNA expression and protein abundance of the epithelial Mg²⁺ channel Trpm6 in *NCC*^{+/+} and *NCC*^{-/-} mice. (A) Renal mRNA expression levels of the epithelial Mg²⁺ channel Trpm6 were determined by real-time quantitative PCR analysis and are depicted as the ratio to HPRT. (B) Trpm6 protein abundance was determined by computerized analysis of immunohistochemical images and is presented as integrated optical density (AU). *n* = 6 animals per genotype. Data are presented as mean ± SEM. **P* < 0.05 versus *NCC*^{+/+} mice.

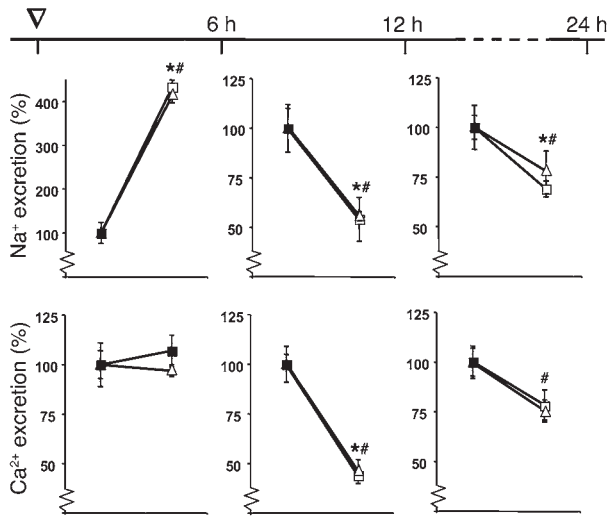


Figure 5
Time-dependent effects of HCTZ on urinary Na⁺ and Ca²⁺ excretion in *Trpv5*^{+/+} and *Trpv5*^{-/-} mice. *Trpv5*^{+/+} and *Trpv5*^{-/-} mice were housed in metabolic cages, and urine was sampled 6, 12, and 24 hours after the intraperitoneal administration of vehicle or 25 mg/kg HCTZ. Arrowhead indicates administration of a single dose of 25 mg/kg HCTZ. Filled squares, vehicle-treated *Trpv5*^{+/+}; open squares, HCTZ-treated *Trpv5*^{+/+}; filled triangles, vehicle-treated *Trpv5*^{-/-}; open triangles, HCTZ-treated *Trpv5*^{-/-}. *n* = 9 animals per treatment group. Data are presented as mean ± SEM; absolute values were normalized to respective vehicle-treated controls. **P* < 0.05 versus vehicle-treated *Trpv5*^{+/+} mice. #*P* < 0.05 versus vehicle-treated *Trpv5*^{-/-} mice.

1.6% ± 0.3% vs. 4.4% ± 1.0%). Since K⁺ secretion occurs along the distal part of the nephron accessible to micropuncture (together with water reabsorption in the CNT and cortical collecting duct [CCD]), the distal luminal concentration of K⁺ was used as an indicator of the distal collection site. Consistent with intact Ca²⁺ reabsorption along the distal convoluted and confirming previous experiments which related fractional Ca²⁺ delivery in distal convoluted to luminal K⁺ concentration (24), both HCTZ-treated and control mice showed a rapid fall in fractional Ca²⁺ delivery with increasing luminal concentrations of K⁺ (Figure 6B). The fractional delivery of Ca²⁺ to the early distal convoluted, identified by low tubular fluid K⁺ concentrations, however, appeared reduced in HCTZ-treated versus control mice (about 4% vs. 10%). This indicates that the Ca²⁺-sparing effect of chronic HCTZ administration localizes upstream to the distal convoluted accessible to micropuncture, i.e. proximal to the site of *Trpv5*-mediated active Ca²⁺ reabsorption (24).

Discussion

The present study demonstrates that enhanced passive Ca²⁺ transport in the proximal tubule due to ECV contraction explains the hypocalcemia that develops during chronic thiazide treatment. Of crucial importance is that micropuncture experiments in HCTZ-treated mice demonstrated increased reabsorption of Na⁺ and Ca²⁺ in the proximal tubule, whereas Ca²⁺ reabsorption in the distal convoluted accessible to micropuncture, which includes the site of *Trpv5*-mediated active Ca²⁺ reabsorption, was unaffected. Furthermore, we showed that thiazide-induced hypocalcemia can be elicited in *Trpv5*^{-/-} mice, in which active Ca²⁺ reabsorption is abolished. In line with these data, we showed that the hypocal-

ciuric response to thiazides parallels a compensatory increase in renal Na⁺ reabsorption secondary to an initial natriuresis. Chronic thiazide administration enhanced Mg²⁺ excretion and specifically reduced renal expression levels of the epithelial Mg²⁺ channel *Trpm6*. In addition, *Trpm6* expression was severely decreased in *NCC*^{-/-} mice. Therefore, the pathogenesis of hypomagnesemia in chronic thiazide treatment as well as Gitelman syndrome appears to involve *Trpm6* downregulation.

ECV contraction is a known stimulus for paracellular Ca²⁺ reabsorption in the proximal tubule (2, 14). Hypovolemia triggers a compensatory increase of proximal Na⁺ reabsorption, which in turn enhances the electrochemical gradient driving passive Ca²⁺ transport in proximal tubular segments (1, 2, 14). HCTZ-treated mice exhibited a significant increase in hematocrit and concomitant decrease in body weight compared with nontreated controls, which confirms that ECV contraction occurred. Importantly, micropuncture experiments showed that HCTZ increases Ca²⁺ reabsorption in the proximal tubule, which results in decreased Ca²⁺ delivery to the last surface loop of the proximal tubule and to the first surface loop of the distal convoluted. This was associated with an increased fractional Na⁺ reabsorption rate in the proximal tubule, as further substantiated by the reduced C_{Li} in HCTZ-treated mice. In line with these data, chronic HCTZ treatment upregulated expression of *NHE3*, which is responsible for the majority of Na⁺ reabsorption in proximal tubules and thus provides the main driving force for passive Ca²⁺ reabsorption. Alternatively, thiazide-induced hypocalcemia has been previously attributed to increased active Ca²⁺ reabsorption. However, the *in vivo* micropuncture experiments indicated similar or even reduced absolute Ca²⁺ reabsorption along the accessible distal convoluted of HCTZ-treated versus control mice, whereas Ca²⁺ delivery to the early accessible distal convoluted was decreased by HCTZ treatment. Previous micropuncture studies in distal convolutions of mice lacking *Trpv5* revealed that Ca²⁺ reabsorption

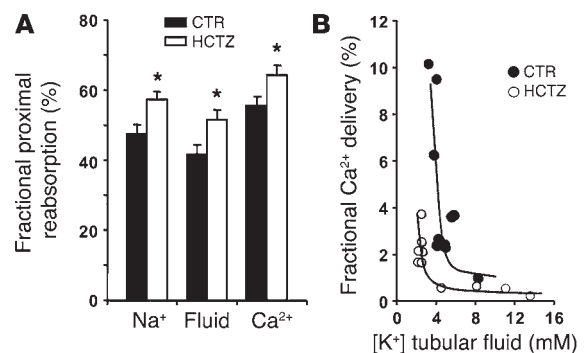


Figure 6
Effect of chronic HCTZ treatment in mice on Ca²⁺ transport along the single nephron assessed by *in vivo* free-flow micropuncture. (A) Fractional reabsorption of Na⁺, fluid, and Ca²⁺ up to the last surface loop of the proximal tubule. (B) Relation between K⁺ concentration in tubular fluid of distal convoluted and fractional Ca²⁺ delivery to these sites. Low K⁺ concentrations indicate early puncture sites, and high K⁺ concentrations indicate late puncture sites of distal convoluted. Black bars and filled circles, vehicle-treated controls; white bars and open circles, HCTZ, 25 mg/kg/d during 6 days. *n* = 10 nephrons for distal collections and *n* = 17–21 nephrons for proximal collections in 5–6 mice per treatment group. Data are presented as mean ± SEM. **P* < 0.05 versus vehicle-treated controls.



is normal up to the early accessible sites but becomes abolished along the downstream accessible segments of distal convolution (24). This indicated that no Trpv5-mediated Ca^{2+} reabsorption occurs upstream to the early sites accessible to micropuncture, which is consistent with the localization of Trpv5 in DCT2 and the CNT (17, 24). Thus, the reduced delivery of Ca^{2+} to the early accessible distal convolution in HCTZ-treated mice cannot be the result of Trpv5-mediated active Ca^{2+} reabsorption. In accordance with these findings, chronic HCTZ administration still decreased urinary Ca^{2+} excretion in mice lacking Trpv5, in which active Ca^{2+} transport in the distal convolution is effectively abolished (24). This is further exemplified by the severe downregulation of the remaining Ca^{2+} transport proteins in *Trpv5*^{-/-} mice, which was unaffected by HCTZ treatment. Together with the micropuncture data, these results indicate that the Ca^{2+} -sparing effect of thiazides can be explained neither by increased Ca^{2+} entry through Trpv5 nor by enhanced active Ca^{2+} transport in general. Additional experiments investigating the time dependency of these HCTZ effects demonstrated that Ca^{2+} excretion is unaltered during the natriuretic response following HCTZ administration, again indicating that direct stimulation of active Ca^{2+} reabsorption by inhibition of NCC does not occur. In contrast, a profound decrease in urinary Ca^{2+} excretion followed the initial natriuresis and, importantly, paralleled a reduced net Na^+ excretion. In line with the present data, we previously demonstrated that volume contraction mimics thiazide-induced hypocalciuria and volume repletion completely reverses this hypocalciuria in rats (7). In conclusion, these data demonstrate that enhanced proximal tubular Na^+ transport, as a consequence of ECV contraction, stimulates paracellular Ca^{2+} transport and constitutes the molecular mechanism underlying thiazide-induced hypocalciuria.

Gitelman syndrome is an autosomal recessive disorder caused by loss-of-function mutations in the gene encoding NCC, with a phenotype resembling chronic thiazide administration (4, 11). Loffing et al. recently demonstrated that renal Trpv5 and NCX1 expression are unaffected in *NCC*^{-/-} mice, which display hypocalciuria (25, 27). Accordingly, micropuncture experiments in *NCC*^{-/-} mice showed that active Ca^{2+} reabsorption is unaltered in distal convolution but that fractional absorption of both Na^+ and Ca^{2+} in the proximal tubule is increased (27). The latter observation is in line with the enhancement of passive Ca^{2+} reabsorption through increased Na^+ reabsorption in the proximal tubule, with results similar to the micropuncture data obtained during chronic HCTZ treatment in the present study. Taken together, our studies demonstrate that increased passive Ca^{2+} reabsorption in the proximal tubule explains the Ca^{2+} -sparing effect of both NCC inhibition and inactivation.

Previously, we showed that thiazide-induced hypocalciuria occurs in spite of reduced renal expression of Ca^{2+} transport proteins in the rat (7). In these experiments a significantly higher dose of HCTZ was administered compared with that in the present study. Loffing et al. previously showed structural damage to and loss of DCT cells during thiazide administration with equivalently high doses, and, therefore, we hypothesized that apoptosis explains the reduced expression levels (7, 26). However, this was never observed in thiazide-treated mice. In the past, we have tried to reproduce the observed apoptotic changes in mice using several mouse strains, both sexes of mice, and different thiazide diuretics and application protocols but were never able to produce any DCT cell apoptosis in mice (J. Loffing, unpublished observations). Accordingly, deleterious effects were not detected in the present

study, and the increased NCC expression in HCTZ-treated animals points to the viability of the DCT (28, 29). However, both studies consistently show that thiazide-induced hypocalciuria persists despite the absence or reduced abundance of proteins essentially responsible for active Ca^{2+} transport.

Interestingly, *Trpv5*^{-/-} mice displayed significant polyuria and acidic urinary pH, which facilitate the excretion of large quantities of Ca^{2+} by reducing the risk of Ca^{2+} precipitations (24, 30–32). HCTZ administration increased diuresis in wild-type animals but did not alter urine volume in *Trpv5*^{-/-} mice. Furthermore, HCTZ normalized the acidic urinary pH in *Trpv5*^{-/-} mice. It has been demonstrated that a high luminal Ca^{2+} concentration, by activating the Ca^{2+} -sensing receptor in the apical membrane of the collecting duct, blunts water permeability through aquaporin-2 (33, 34). Therefore, the Ca^{2+} -sparing effect of HCTZ might counteract the hypercalciuria-induced polyuria and remove the necessity for urine acidification in *Trpv5*^{-/-} mice, which would suggest that the distal Ca^{2+} load directly influences urine volume and acidification in an effort to prevent kidney stone formation.

Hypomagnesemia, as a side-effect of chronic thiazide administration and a defining feature of Gitelman syndrome, remains unexplained. Chronic HCTZ administration increased urinary Mg^{2+} excretion in the presence of reduced serum Mg^{2+} levels while GFR remained unaffected, which confirms that the hypomagnesemia is due to renal Mg^{2+} wasting. Importantly, renal Trpm6 expression was reduced in HCTZ-treated animals, while NCC expression was enhanced, which illustrates that Trpm6 downregulation is a specific nondeleterious effect. Trpm6 constitutes a Mg^{2+} -permeable channel localized along the apical membrane of the DCT to which active Mg^{2+} reabsorption is restricted (21–23). Mutations in Trpm6 were shown to be associated with renal Mg^{2+} wasting (21, 22). Furthermore, we previously demonstrated a similarly reduced Trpm6 expression in tacrolimus-induced hypomagnesemia (35). Thus, the present data suggested that chronic thiazide treatment results in a similar defect in active Mg^{2+} reabsorption. As Trpm6 and NCC exactly colocalize in the DCT, a direct inhibitory effect of decreased NaCl influx on active Mg^{2+} transport could in principle be involved (23). However, whereas Ca^{2+} reabsorption was diminished upon a single dose of HCTZ, urinary Mg^{2+} excretion remained unaltered within 24 hours after HCTZ administration, which contradicts the hypothesis that Mg^{2+} reabsorption is directly inhibited. This dissociation of Ca^{2+} and Mg^{2+} excretion can be explained when the relative contribution of the proximal tubule and the TAL in the passive reabsorption of these divalents is taken into account. The majority of Mg^{2+} is reabsorbed in the TAL due to the driving force generated by NKCC2-mediated NaCl reabsorption, while micropuncture studies have shown that thiazides particularly enhance proximal tubule Na^+ transport (14, 36). Accordingly, we showed that HCTZ increases proximal tubular NHE3 expression without affecting the NKCC2 expression. Hypothetically, an additional defect of Mg^{2+} reabsorption in TAL could explain the increased Mg^{2+} excretion in HCTZ treatment. However, inborn as well as acquired defects in TAL Mg^{2+} reabsorption are consistently accompanied by hypercalciuria, which renders this hypothesis unfeasible when the Ca^{2+} -sparing effect of thiazides is taken into account (37–40). In line with the data obtained during HCTZ administration, *NCC*^{-/-} mice were also shown to display hypomagnesemia in the absence of hypokalemia (4, 25). In the present study we report that, similar to what occurs during chronic thiazide administration, renal Trpm6 abundance in the



DCT is significantly reduced in *NCC*^{-/-} mice. Therefore, *Trpm6* downregulation may represent a general mechanism involved in the pathogenesis of hypomagnesemia in both Gitelman syndrome and chronic thiazide administration.

NCC^{-/-} mice were previously shown to display widespread atrophy of DCT cells (27). This marked reduction in DCT plasma membrane area and, thereby, apical expression of Mg^{2+} channels could explain the observed renal Mg^{2+} wasting. As discussed above, deleterious effects of chronic thiazide administration particularly on DCT1 were previously suggested but did not occur in the present study (7, 26). Thus, at present it is unknown which mechanism is responsible for the observed *Trpm6* downregulation. In this respect, it is interesting to note that aldosterone excess has been shown to be associated with renal Mg^{2+} wasting, whereas hypermagnesemia may accompany aldosterone deficiency (4, 41). In addition, it has been shown that the mineralocorticoid receptor antagonist spironolactone reduces urinary Mg^{2+} excretion in patients with Gitelman syndrome (42, 43). During thiazide-induced ECV contraction as well as in *NCC*^{-/-} mice, aldosterone levels are increased (25). Therefore, hyperaldosteronism might hypothetically downregulate *Trpm6* expression and, thereby, result in renal Mg^{2+} wasting.

In conclusion, this study addressing the mechanism underlying thiazide-induced hypocalciuria answers a long-standing question in physiology and medicine. Furthermore, it offers new insights concerning the hypomagnesemia accompanying chronic thiazide treatment and Gitelman syndrome.

Methods

Animal studies in *Trpv5*^{-/-} and *NCC*^{-/-} mice

Experiment 1. *Trpv5*^{-/-} mice were recently generated by targeted ablation of the *Trpv5* gene (24). In short, the *Trpv5* gene was cloned from a 129/Sv mouse genomic library and subcloned in a modified neomycin-*loxP*-targeting vector. Eventually, a recombinant ES cell line was used to generate chimeras, which allowed germline transmission of the mutant allele (*Trpv5*^{loxneo}). Heterozygous (*Trpv5*^{+/+}) mice, harboring 1 null allele, were obtained by breeding *Trpv5*^{loxneo} mice with a germline *Ella-cre*-deletor strain (44). The offspring of *Trpv5*^{+/+} mice were genotyped by PCR as described previously (44). Eight-week old male *Trpv5*^{+/+} and *Trpv5*^{-/-} littermates were kept in a light- and temperature-controlled room with ad libitum access to deionized drinking water and standard pelleted chow (0.25% [wt/vol] NaCl; 1% [wt/vol] Ca; 0.2% [wt/vol] Mg). Mice were randomly assigned to either the control or HCTZ treatment group. Control animals received daily intraperitoneal injections of vehicle only. HCTZ was administered by intraperitoneal injection of 25 mg/kg/d. Mice were treated for 6 days, after which they were housed in metabolic cages, which enabled 24-hour collection of urine samples. At the end of the experiment, blood samples were taken, and the animals were sacrificed. Subsequently, kidney and duodenum were sampled.

Experiment 2. A second metabolic study was performed to study the effects of a single dose of HCTZ at various time intervals after administration. To this end, *Trpv5*^{+/+} and *Trpv5*^{-/-} littermates were housed in metabolic cages, and urine was collected 6, 12, and 24 hours after administration of vehicle. One week later, the mice were intraperitoneally injected with a single dose of 25 mg/kg HCTZ. Likewise, urine was collected 6, 12, and 24 hours thereafter, which enabled analysis of the time-dependent effects of HCTZ on Na^+ , Ca^{2+} , and Mg^{2+} excretion.

Experiment 3. *NCC*^{-/-} mice were generated and characterized as described previously by Schultheis et al. (25). *NCC*^{+/+} and *NCC*^{-/-} mice had ad libitum

access to drinking water and standard pelleted chow (0.24% [wt/vol] NaCl; 1% [wt/vol] Ca; 0.2% [wt/vol] Mg); after animals were sacrificed, kidneys were sampled for determination of renal *Trpm6* mRNA expression and protein abundance. The animal ethics board of the Radboud University Nijmegen Medical Centre approved the animal studies.

Analytical procedures

We determined serum and urine Ca^{2+} and Mg^{2+} concentrations using a colorimetric assay as described previously (45). We measured serum and/or urine Na^+ , Cl^- , K^+ , and creatinine concentrations using a Hitachi autoanalyzer (Hitachi Corp.). A flame spectrophotometer (FCM 6343; Eppendorf) was used to measure serum and urine Li^+ concentrations. We determined hematocrit using a standard centrifugation protocol (46).

Real-time quantitative PCR

Total RNA was extracted from kidney and duodenum and reverse transcribed as described previously (7, 47). The obtained cDNA was used to determine *Trpv5*, calbindin-*D*_{28K}, *NCX1*, *Trpm6*, *NKCC2*, and hypoxanthine-guanine phosphoribosyl transferase mRNA levels in kidney by real-time quantitative PCR, as described previously (48). *NKCC2* forward and reverse primer sequences, respectively, were 5'-CCTATGTGAGTGCTTAGACAACGCTCTGGA-3' and 5'-GGCTCCTCCACACAGGCTC-3', and the sequence for the fluorescent probe (5'-FAM-3'-TAMRA) was 5'-CACATGGTCTTCCACTGTGGTT-3'. In the case of *Trpm6*, these were 5'-CCTGTCTGAGGATGATGTTCTCAAGCC-3', 5'-AAAGCCATGCGAGTTATCAGC-3', and 5'-CTTCACAATGAAAACCTGCC-3'.

Immunohistochemistry and immunoblotting

Staining of kidney sections for *Trpv5*, calbindin-*D*_{28K}, *Trpm6*, *NCC*, and *NHE3* was performed on 7- μ m cryosections of periodate-lysine-paraformaldehyde-fixed kidney samples. Sections were stained with guinea pig anti-*Trpv5* (17), mouse anti-calbindin-*D*_{28K} (Swant), affinity-purified guinea pig anti-*Trpm6* (23), rabbit anti-*NCC* (7), and rabbit anti-*NHE3* (49), as described previously (24, 35). Images were made using a Zeiss fluorescence microscope equipped with a digital photo camera (DMX1200; Nikon). For semiquantitative determination of protein levels, images were analyzed with the Image-Pro Plus 4.1 image analysis software (MediaCybernetics), and protein levels were quantified as the mean of integrated optical density. Of note, in the case of *NHE3* specifically, the immunopositive signal in kidney cortex was quantified, which represents proximal tubular *NHE3* expression. Semiquantitative immunoblotting for calbindin-*D*_{28K} and *NCC* was performed as described previously (7). Immunopositive bands were scanned and pixel density was determined using the Image-Pro 4.1 image analysis software.

In vivo free-flow micropuncture experiments in HCTZ-treated wild-type mice

Male C57BL/6 mice were randomly assigned to control or chronic HCTZ treatment as described in experiment 1. After day 6 of treatment, the left kidney was prepared for renal micropuncture under inactin/ketamine anesthesia as described previously (50). For assessment of single nephron glomerular filtration rate, [³H]inulin was infused intravenously. On the kidney surface, the last loop of proximal tubules or the distal convolutions was identified and punctured for quantitative collections of tubular fluid. Tubular fluid volumes were determined from column length in a constant-bore capillary. The concentrations in tubular fluid of Na^+ and K^+ were determined by a micro-flame photometer (Department of Pharmacology, University of Tübingen, Germany) (24, 27) and of Ca^{2+} by a flow-through microfluorometer (NanoFlo; World Precision Instruments Inc.) using Fluo-3 (MoBiTec) for detection (24, 27).



Statistical analysis

Data are expressed as mean ± SEM. Statistical comparisons were analyzed by 1-way ANOVA and Fisher multiple comparison. *P* < 0.05 was considered statistically significant. All analyses were performed using the StatView Statistical Package software (Power PC version 4.5.1; Abacus Concepts Inc.) on an iMac computer (Apple Computer Inc.).

Acknowledgments

The work presented in this article was financially supported by the Dutch Kidney Foundation (C10.1881, C03.6017) and the Dutch Organization of Scientific Research (Zon-Mw 016.006.001). The authors wish to thank O.W. Moe (University of Texas Southwestern

Medical Center, Dallas, Texas, USA) for generously providing the NHE3 antibody and K. Richter (University of California and Veterans Affairs Medical Center) and the Central Animal Facility (Radboud University Nijmegen Medical Centre) for expert technical assistance.

Received for publication December 9, 2004, and accepted in revised form April 12, 2005.

Address correspondence to: René J.M. Bindels, 160 Cell Physiology, Radboud University Nijmegen Medical Centre, PO Box 9101, NL-6500 HB Nijmegen, The Netherlands. Phone: 31-24-3614211; Fax: 31-24-3616413; E-mail: r.bindels@ncmls.ru.nl.

1. Monroy, A., Plata, C., Hebert, S.C., and Gamba, G. 2000. Characterization of the thiazide-sensitive Na⁺-Cl⁻ cotransporter: a new model for ions and diuretics interaction. *Am. J. Physiol. Renal Physiol.* **279**:F161-F169.
2. Hoenderop, J.G.J., Nilius, B., and Bindels R.J.M. 2005. Calcium absorption across epithelia. *Physiol. Rev.* **85**:373-422.
3. Costanzo, L.S., and Windhager, E.E. 1978. Calcium and sodium transport by the distal convoluted tubule of the rat. *Am. J. Physiol.* **235**:F492-F506.
4. Ellison, D.H. 2000. Divalent cation transport by the distal nephron: insights from Bartter's and Gitelman's syndromes. *Am. J. Physiol. Renal Physiol.* **279**:F616-F625.
5. Reilly, R.F., and Ellison, D.H. 2000. Mammalian distal tubule: physiology, pathophysiology, and molecular anatomy. *Physiol. Rev.* **80**:277-313.
6. Dai, L.J., et al. 2001. Magnesium transport in the renal distal convoluted tubule. *Physiol. Rev.* **81**:51-84.
7. Nijenhuis, T., et al. 2003. Thiazide-induced hypocalcemia is accompanied by a decreased expression of Ca²⁺ transport proteins in kidney. *Kidney Int.* **64**:555-564.
8. Ray, W.A., Griffin, M.R., Downey, W., and Melton, L.J. 1989. Long-term use of thiazide diuretics and risk of hip fracture. *Lancet.* **1**:687-690.
9. Reid, I.R., et al. 2000. Hydrochlorothiazide reduces loss of cortical bone in normal postmenopausal women: a randomized controlled trial. *Am. J. Med.* **109**:362-370.
10. LaCroix, A.Z., et al. 1990. Thiazide diuretic agents and the incidence of hip fracture. *N. Engl. J. Med.* **322**:286-290.
11. Gitelman, H.J., Graham, J.B., and Welt, L.G. 1966. A new familial disorder characterized by hypokalemia and hypomagnesemia. *Trans. Assoc. Am. Physicians.* **79**:221-235.
12. Lemmink, H.H., et al. 1996. Linkage of Gitelman syndrome to the thiazide-sensitive sodium-chloride cotransporter gene with identification of mutations in Dutch families. *Pediatr. Nephrol.* **10**:403-407.
13. Nijenhuis, T., Hoenderop, J.G., Nilius, B., and Bindels, R.J. 2003. (Patho)physiological implications of the novel epithelial Ca²⁺ channels TRPV5 and TRPV6. *Pflügers Arch.* **446**:401-409.
14. Walter, S.J., and Shirley, D.G. 1986. The effect of chronic hydrochlorothiazide administration on renal function in the rat. *Clin. Sci. (Lond.)* **70**:379-387.
15. Friedman, P.A. 1998. Codependence of renal calcium and sodium transport. *Annu. Rev. Physiol.* **60**:179-197.
16. Friedman, P.A., and Bushinsky, D.A. 1999. Diuretic effects on calcium metabolism. *Semin. Nephrol.* **19**:551-556.
17. Hoenderop, J.G., et al. 2000. Localization of the epithelial Ca²⁺ channel in rabbit kidney and intestine. *J. Am. Soc. Nephrol.* **11**:1171-1178.
18. Biner, H.L., et al. 2002. Human cortical distal nephron: distribution of electrolyte and water transport pathways. *J. Am. Soc. Nephrol.* **13**:836-847.
19. Loffing, J., et al. 2001. Distribution of transcellular calcium and sodium transport pathways along mouse distal nephron. *Am. J. Physiol. Renal Physiol.* **281**:F1021-F1027.
20. Quamme, G.A. 1997. Renal magnesium handling: new insights in understanding old problems. *Kidney Int.* **52**:1180-1195.
21. Schlingmann, K.P., et al. 2002. Hypomagnesemia with secondary hypocalcemia is caused by mutations in TRPM6, a new member of the TRPM gene family. *Nat. Genet.* **31**:166-170.
22. Walder, R.Y., et al. 2002. Mutation of TRPM6 causes familial hypomagnesemia with secondary hypocalcemia. *Nat. Genet.* **31**:171-174.
23. Voets, T., et al. 2004. TRPM6 forms the Mg²⁺ influx channel involved in intestinal and renal Mg²⁺ absorption. *J. Biol. Chem.* **279**:19-25.
24. Hoenderop, J.G., et al. 2003. Renal Ca²⁺ wasting, hyperabsorption, and reduced bone thickness in mice lacking TRPV5. *J. Clin. Invest.* **112**:1906-1914. doi:10.1172/JCI200319826.
25. Schultheis, P.J., et al. 1998. Phenotype resembling Gitelman's syndrome in mice lacking the apical Na⁺-Cl⁻ cotransporter of the distal convoluted tubule. *J. Biol. Chem.* **273**:29150-29155.
26. Loffing, J., et al. 1996. Thiazide treatment of rats provokes apoptosis in distal tubule cells. *Kidney Int.* **50**:1180-1190.
27. Loffing, J., et al. 2004. Altered renal distal tubule structure and renal Na⁺ and Ca²⁺ handling in a mouse model for Gitelman's syndrome. *J. Am. Soc. Nephrol.* **15**:2276-2288.
28. Chen, Z.F., Vaughn, D.A., Beaumont, K., and Fanesitl, D.D. 1990. Effects of diuretic treatment and of dietary sodium on renal binding of ³H-metolazone. *J. Am. Soc. Nephrol.* **1**:91-98.
29. Morsing, P., Velazquez, H., Wright, F.S., and Ellison, D.H. 1991. Adaptation of distal convoluted tubule of rats. II. Effects of chronic thiazide infusion. *Am. J. Physiol.* **261**:F137-F143.
30. Miller, L.A., and Stapleton, F.B. 1989. Urinary volume in children with urolithiasis. *J. Urol.* **141**:918-920.
31. Frick, K.K., and Bushinsky, D.A. 2003. Molecular mechanisms of primary hypercalciuria. *J. Am. Soc. Nephrol.* **14**:1082-1095.
32. Baumann, J.M. 1998. Stone prevention: why so little progress? *Urol. Res.* **26**:77-81.
33. Sands, J.M., et al. 1997. Apical extracellular calcium/polyvalent cation-sensing receptor regulates vasopressin-elicited water permeability in rat kidney inner medullary collecting duct. *J. Clin. Invest.* **99**:1399-1405.
34. Puliyaanda, D.P., Ward, D.T., Baum, M.A., Hammond, T.G., and Harris, H.W., Jr. 2003. Calpain-mediated AQP2 proteolysis in inner medullary collecting duct. *Biochem. Biophys. Res. Commun.* **303**:52-58.
35. Nijenhuis, T., Hoenderop, J.G., and Bindels, R.J. 2004. Downregulation of Ca²⁺ and Mg²⁺ transport proteins in the kidney explains tacrolimus (FK506)-induced hypercalciuria and hypomagnesemia. *J. Am. Soc. Nephrol.* **15**:549-557.
36. Fisher, K.A., et al. 2001. Regulation of proximal tubule sodium/hydrogen antiporter with chronic volume contraction. *Am. J. Physiol. Renal Physiol.* **280**:F922-F926.
37. Simon, D.B., et al. 1999. Paracellin-1, a renal tight junction protein required for paracellular Mg²⁺ resorption. *Science.* **285**:103-106.
38. Weber, S., et al. 2000. Familial hypomagnesemia with hypercalciuria and nephrocalcinosis maps to chromosome 3q27 and is associated with mutations in the PCLN-1 gene. *Eur. J. Hum. Genet.* **8**:414-422.
39. Simon, D.B., et al. 1996. Bartter's syndrome, hypokalaemic alkalosis with hypercalciuria, is caused by mutations in the Na-K-2Cl cotransporter NKCC2. *Nat. Genet.* **13**:183-188.
40. Blanchard, A., et al. 2001. Paracellin-1 is critical for magnesium and calcium reabsorption in the human thick ascending limb of Henle. *Kidney Int.* **59**:2206-2215.
41. Horton, R., and Biglieri, E.G. 1962. Effect of aldosterone on the metabolism of magnesium. *J. Clin. Endocrinol. Metab.* **22**:1187-1192.
42. Stergiou, G.S., Mayopoulou-Symvoulidou, D., and Mountokalakis, T.D. 1993. Attenuation by spironolactone of the magnesium effect of acute furosemide administration in patients with liver cirrhosis and ascites. *Miner. Electrolyte Metab.* **19**:86-90.
43. Colussi, G., Rombola, G., De Ferrari, M.E., Macaluso, M., and Minetti, L. 1994. Correction of hypokalemia with anti-aldosterone therapy in Gitelman's syndrome. *Am. J. Nephrol.* **14**:127-135.
44. Lakso, M., et al. 1996. Efficient in vivo manipulation of mouse genomic sequences at the zygote stage. *Proc. Natl. Acad. Sci. U. S. A.* **93**:5860-5865.
45. Hoenderop, J.G.J., et al. 2001. Calcitriol controls the epithelial calcium channel in kidney. *J. Am. Soc. Nephrol.* **12**:1342-1349.
46. Sirs, J.A. 1968. The measurement of the haematocrit and flexibility of erythrocytes with a centrifuge. *Biorheology.* **5**:1-14.
47. Van Abel, M., et al. 2002. 1,25-Dihydroxyvitamin D₃-independent stimulatory effect of estrogen on the expression of ECaC1 in the kidney. *J. Am. Soc. Nephrol.* **13**:2102-2109.
48. Hoenderop, J.G.J., et al. 2002. Modulation of renal Ca²⁺ transport protein genes by dietary Ca²⁺ and 1,25-dihydroxyvitamin D₃ in 25-hydroxyvitamin D₃-1(alpha)-hydroxylase knockout mice. *FASEB J.* **16**:1398-1406.
49. Amemiya, M., et al. 1995. Expression of NHE-3 in the apical membrane of rat renal proximal tubule and thick ascending limb. *Kidney Int.* **48**:1206-1215.
50. Vallon, V. 2003. In vivo studies of the genetically modified mouse kidney. *Nephron. Physiol.* **94**:1-5.